SciencePG
Science Publishing Group

Distinct Embryonic and Adult Fates of Multipotent Myogenic Progenitors Isolated from Skeletal Muscle and Bone Marrow

Zhuqing Qu-Petersen[1], Jesper L. Andersen[2], Shi Zhou[3]

[1]The Copenhagen Muscle Research Center, National University Hospital, Copenhagen, Denmark
[2]Institute of Sports Medicine and Center for Healthy Aging, University of Copenhagen, Bispebjerg Hospital, Copenhagen, Denmark
[3]School of Health and Human Sciences, Southern Cross University, Lismore, Australia

Email address:
zhuqing.qu.petersen@rh.regionh.dk (Zhuqing Qu-Petersen)

Abstract: Identification of multipotent progenitors has been difficult due to their rarity in adults. Here, we report a novel type of neuroepithelial myogenic progenitor that can be isolated from adult murine skeletal muscle. In culture, these progenitors generated radial glia-like cells that initiated mosaic myotubes, and subsequently developed into embryonic/fetal-like myoblasts capable of robust myofiber formation. These cells could also differentiate into neuronal lineage. By contrast, progenitors from bone marrow produced progenies more uniformly of an adult myoblast lineage. When grafted into dystrophic muscles of mdx mice, the muscle- and marrow-derived cells restored dystrophin expression; however, fetal-like myogenesis towards a defective adult fate was demonstrated in the muscle-derived cells. This impaired regenerative capacity resembled Duchenne muscular dystrophy patients, suggesting a potential connection between the neuroepithelial myogenic progenitor and the etiology of this myopathy. The distinct fates of the two types of progenitors imply their different roles in muscle regeneration and pathogenesis.

Keywords: Neuroepithelial Myogenic Progenitors, Bone Marrow Myogenic Cells, Neural Differentiation, Myogenesis, Cell Transplantation, Muscular Dystrophy

1. Introduction

Isolation and identification of purified multipotent progenitor/stem cells from postnatal tissues have become a major focus of basic and clinical investigations [1, 2]. These cells can provide a range of tissue-specific progenitors for repair of damaged tissues or modeling human disease [3, 4]. Over the past decade, different tissue-associated progenitor cells have been isolated, and tested for muscle regeneration, especially in the animal models of Duchenne muscular dystrophy (DMD) [5–11]. DMD is the most common and severe form of congenital muscle disease, in which the absence of dystrophin in the membrane of myofibers results in muscle fiber necrosis and progressive muscle weakness [12]. Stem cell therapy may provide the opportunity to restore dystrophin expression and replace the damaged muscle tissue [13, 14]. To date, the efficiency of initial grafting myoblasts or muscle satellite cells is too low to meet therapeutic objectives, and the recent advances in the strategies have encountered different challenges [13, 14].

Adult bone marrow has been considered as accessible sources for isolation of multipotent myogenic progenitors. A side population (SP cells) sorted by their ability to efflux the Hoechst dye and mesenchymal stromal cells (MSCs) separated as adherent cells in culture or by lineage markers, have been tested for muscle differentiation [5, 7, 8, 11]. However, poor engraftments have resulted from transplantation of bone marrow-derived cells, including SP cells and MSCs into dystrophic mice [5, 8, 15]. More immature subpopulations of myogenic progenitors sorted by pre-defined cell surface markers from skeletal muscle are able to contribute to the satellite cell pool and give improved engraftments in dystrophin-deficient *mdx* mice [16–18]. Different populations of myogenic cells have also been derived from vascular progenitor cells [9], adipose-derived progenitors [10], genetically modified mesenchymal stem cells [19], and embryonic stem cells [20]. While the efficiency of engraftments is improving, muscle function has

been limited, and variable [21, 22], and tumorigenesis has been reported in studies [19, 20]. These outcomes raise critical issues about the heterogeneity of the original progenitor cells transplanted and the physiological role of multipotent progenitors in muscle regeneration.

Most of the investigations have focused on the development of adult myogenic progenitor/stem cells for use in cell replacement therapy. Indirect evidence from human pathology, however, suggests the presence of more immature progenitors in postnatal tissues. For example, despite the origin of single cells, both neuroblastoma and rhabdomyosarcoma contain embryonic-like tissues with muscle and neural cell phenotypes [23]. This suggests that a rare number of primitive myogenic cells may exist in postnatal tissues, and function differently from tissue-specific progenitor/stem cells. Identification of these primitive progenitors is crucial when considering the proposed therapeutic roles of multipotent cells in regenerative medicine. In addition, understanding of the basic biology of the immature progenitors may provide insights into the cellular origin of human diseases [3, 4, 24]. Because of the low frequency of these cells in adults, isolation and identification of purified primitive cells in a given tissue have been difficult.

In the present study, we aimed to isolate purified primary colonies of multipotent progenitors with myogenic potential from adult skeletal muscle. To test whether myogenic progenitors could be obtained from other sources, we also isolated primary colonies from bone marrow by similar approaches. We report in this paper the identification and characterization of the most primitive cells from normal murine skeletal muscle, termed neuroepithelial myogenic progenitors (NEMPs), by comparing their marker profiles, myogenic/neurogenic potential, and transplantation capacity with myogenic cells isolated from bone marrow (BMMCs).

2. Experimental Procedures

2.1. Cell Isolation

NEMPs were isolated from the hindlimb muscle of normal C57BL/6 mice (five weeks old) by clonal isolation. A subset of suspension cells was first collected from primary muscle cultures at isolation day 5, using a modified preplate technique reported previously [6, 25, 26]. The suspension cells were then seeded at a clonal density (15–30 cells/cm^2) in culture wells, and developed primary colonies in two weeks. NEMPs were originally from three primary colonies, presumably three primitive NEMP cells. The frequency of the primary NEMP colonies is one in 130 mg hindlimb muscle (from five independent isolations). Two primary clonal populations of NEMP-c1 and NEMP-c2 were established by two times of cloning to confirm single cell nature of the NEMP colonies. BMMCs were isolated from the femurs of normal mice (seven weeks old) by similar technique of preplate and clonal isolation used for NEMP cells, except that the marrow cells were treated with the

supernatant of muscle extract before progressing preplate. We filtered the supernatant and checked no cells in it. The frequency of BMMC colony is approximately one per 10^5–10^6 marrow cells. All the cell populations were of female origin except the NEMP-c1, which was deliberately derived from male mice. The detailed information for isolation can be found in supplementary information.

2.2. Cell Growth

Each primary clone/colony contained 50–100 cells, and thus expansion of these cells was carried out and was set as passage 1 (P$_1$). The NEMP populations tended to differentiate and fuse rapidly in the early cultures. To establish adequate less differentiated cells, the expansion of NEMPs and BMMCs at P$_{1-5}$ was carried out in the growth medium (20% serum) at a density of 0.5–2.5 × 10^3 cells/cm^2. The medium was changed daily. The BMMCs could be expanded at a higher cell density without fusing. The passages at this stage are defined as the times when trypsin was used to detach the cells, starting from the initial expansion of the primary colonies. From P$_6$, the cells were seeded at a cell density of 1.5 × 10^3 cells/cm^2 and passaged when the culture reached ~7.5 × 10^3 cells/cm^2 (NEMPs) and ~1.5 × 10^4 cells/cm^2 (BMMCs). The medium was changed every 2 days. The number of cells per cm^2 was counted at daily intervals for calculating the population doublings, and two culture samples were used for each cell type from P$_6$.

2.3. In Vitro Myofiber Formation

To investigate early spontaneous differentiation, the NEMPs and BMMCs at P$_{3-5}$ were seeded in 12-well plates at a density of 2.5–5 × 10^3 cells/cm^2. After culturing in the growth medium for 5 days, SMMts/myotubes developed and the cells were fixed with cold methanol for immunocytochemistry and myofiber formation. To examine induced myofiber formation, NEMPs and BMMCs at P$_{8-12}$ and P$_{16-20}$ were seeded in 6-well plates and grown to a density of 1.5–2 × 10^4 cells/cm^2. The growth medium was then replaced with differentiation medium (2% horse serum) for 5 days. The cells were fixed and the number of nuclei in myotubes and the total number of nuclei were scored in five random fields (×100) per well. Quantitative analysis of differentiation kinetics was performed in five or six individual trials by measuring the fusion index, which was expressed as the percentage of nuclei incorporated into myotubes [27].

2.4. Cell Transplantation

We grafted BMMCs, NEMPs and NEMP-c1 (P$_{8-12}$) into the gastrocnemius medialis of dystrophin-deficient *mdx* mice (C57BL/10ScSn-Dmd^{mdx}/J, 6–14 weeks old) as single injection. For each muscle, 1.5 × 10^5 or 3 × 10^5 cells, suspended in 15 μl of HBSS (Life Technologies), were used. The total number of cells grafted was varied due to the difficulty in expansion of NEMP myogenic cells. The mice were sacrificed at 14 days or 40–50 days post-grafting and

the entire gastrocnemius muscles were frozen for analysis. BMMCs (5×10^4) were also injected into the irradiated tibialis anterior muscles of *mdx* nu/nu mice and the injected muscles were assessed 35 days after grafting [16].

2.5. Immunohistochemistry and Histochemistry

2.5.1. Dystrophin Immunostaining

Serial cryosections (10 μm) were collected throughout the gastrocnemius muscles. The sections were fixed in acetone for 5 min at -20°C, and blocked in 5% serum or 1% BSA for 30 min at room temperature. For dystrophin staining, sections were incubated with rabbit anti-dystrophin antibody (1:1, Neo Markers) for 30 min and Alexa Fluor 594 (1:500, Life Technologies) for 30 min, and counterstained with Hoechst 33342 (Sigma-Aldrich). The cross sections with the highest number of dystrophin$^+$ fibers were counted in the grafted gastrocnemius medialis. The percentage of CNFs, and the diameter of myofibers were measured from an average of 600 dystrophin$^+$ fibers (172−2141) in between five and 10 sections for each injected muscle. The diameter of dystrophin$^+$ fibers was measured from the short diameter of polygonal myofibers (the relative diameter). For the non-grafted areas, five sections of the gastrocnemius lateralis were counted for the average of dystrophin$^+$ fibers, and an average of 392 and 309 myofibers from three randomly chosen areas were measured for the percentage of CNFs and the diameter of myofibers. To evaluate dystrophin$^-$ fibers in the late grafts, the gastrocnemius medialis with large numbers of small dystrophin$^-$ fibers were used. The percentage of dystrophin$^-$ fibers with peripheral or central nuclei was measured by differential interference contrast (DIC) images merged with dystrophin and Hoechst staining, from an average of 602 dystrophin$^-$ fibers (465−752) in between three and five sections for each grafted muscle.

2.5.2. Developmental Myosin Heavy Chain (Dev-MyHC) and Dystrophin Double Staining

The sections were incubated with anti-dev-MyHC (1:20, Vector Laboratories) for 90 min, and the next steps were performed according to the instructions of M.O.M.^{TM} kit manufacturer (Vector Laboratories). The sections were then stained with anti-dystrophin as described above.

2.5.3. Pax7 and Dystrophin Double Staining

The sections were incubated with mouse anti-Pax7 (1:50, R&D Systems) for 2 h and Alex Fluor 594 goat anti-mouse IgG1 (1:500, Life Technologies) for 1 h. The sections were then stained with anti-dystrophin (1:1, Neo Markers) followed by Alexa Fluor 488 donkey anti-rabbit IgG (1:500, Life Technologies), and counterstained with Hoechst. The number of Pax7$^+$ cells was counted in 15–20 fields (× 200) of both grafted (dystrophin$^+$ fibers) and non-grafted areas (adjacent dystrophin− fibers), in three to six sections of each injected muscle.

2.5.4. Pax7 and Laminin Double Staining

Staining was performed as described above except that anti-dystrophin was replaced by anti-laminin (1:100, Sigma-Aldrich).

2.5.5. MyoD and Dystrophin Double Staining

Staining was performed as described for Pax7 and dystrophin double staining except that anti-Pax7 was replaced by anti-MyoD (1:80, BD Biosciences).

2.5.6. Hematoxylin & Eosin Stain

Staining was performed according to the manufacturer's instructions (Sigma-Aldrich).

2.6. Statistics

Data were presented as mean ± SEM. Student's *t*-test was used to compare differences between NEMPs and BMMCs in expression of the transcripts, the myofiber formation, the population doubling time, and the transplantation capacity. An alpha level of $P \leq 0.05$ was set for statistical significance.

Additional methods (Neural Differentiation, Immunocytochemistry, Flow Cytometry, SDS-PAGE and Western Blotting, Real-Time RT-PCR, NEMP Clone Isolation and In Situ Hybridization) can be found in the supplementary information of the paper.

3. Results

3.1. Cell Populations and Marker Profiles

NEMPs and BMMCs were used in the main analysis of the study. NEMP-c1 and NEMP-c2 were also used in separate experiments due to the small number of primitive NEMP cells. In the growth medium, NEMPs and BMMCs could be propagated for more than 20 passages (Fig. 1A), which is equivalent to 48 (for NEMPs) and 62 population doublings (for BMMCs). Based on our primary focus on the primitive progenitors and their differentiation, the NEMPs at passages 3–6 ($P_{3–6}$), $P_{8–12}$, and $P_{16–20}$, and their BMMC counterparts were analyzed.

We first evaluated the marker profiles in activated primitive (P_3) and more differentiated NEMPs and BMMCs (P_{11}) by quantitative RT-PCR (Fig. 1B). In NEMP-P_3, neural progenitor marker *nestin* [28] was 2.12-fold higher (P < 0.05) than in P_{11}, which fits high expression of *nestin* in neural progenitors and low expression in their differentiated cells. In BMMCs, *Nestin* was low in P_3 and slightly higher in P_{11} (1.38-fold, P > 0.05). Since > 85% of BMMC cells in P_{11} were committed to a myogenic lineage (see below), the increased nestin expression is unlikely related to a neural progenitor phenotype. In P_3, myogenic regulatory factors (MRFs) *MyoD* and *myogenin* were higher in NEMPs than in BMMCs, suggesting NEMP's high potential for myogenic differentiation. In P_{11}, *MyoD* transcript remained at a higher level in NEMPs than in BMMCs. By contrast, *Myf5* transcript, one of the MRFs, was lower in P_3 and up-regulated in P_{11} of both NEMPs and BMMCs. Embryonic muscle progenitor marker *Pax3* [29–31] was observed in NEMP-P_3 and rapidly up-regulated in P_{11}. For BMMCs, although *Pax3* became detectable in all the samples of P_{11}, its

expression was 6-fold higher in NEMPs. In P_3, satellite cell marker *Pax7* was detected in two of four samples of NEMPs and BMMCs. Embryonic stem cell marker *Oct-4* and PNS glial marker *Sox10* were not detected in NEMPs and BMMCs, although *Sox10* was observed in an independent NEMP population (not shown). The data indicate (Fig. 1C)

that activated NEMPs expressed high levels of markers for neural progenitor and muscle lineage (P_3, *nestin*[hi]*MyoD*[hi]*myogenin*[hi]) and differentiated into embryonic-like myogenic cells (P_{11}, *MyoD*[hi]*Myf5*^{hi}*Pax3*^{hi}), but BMMCs displayed more homogeneous myogenic marker profiles in P_3 and P_{11}.
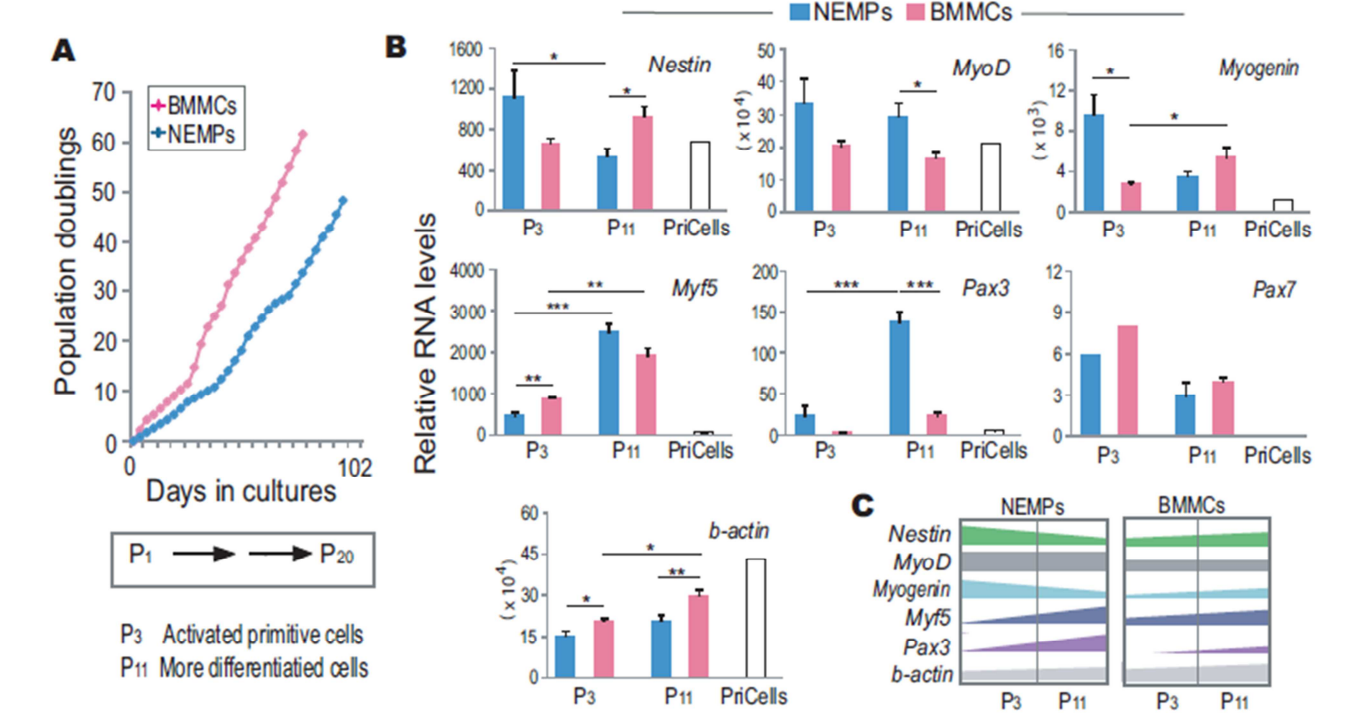

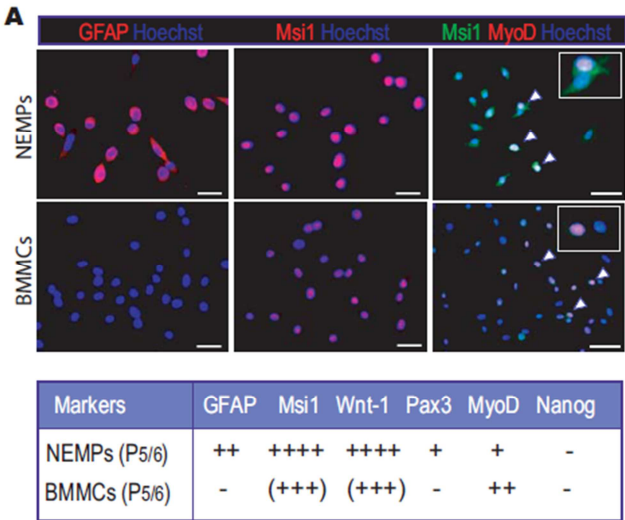***Figure 1.*** *Growth Property and Early Lineage Identification by Quantitative RT-PCR.*

(A) Growth curves of population doublings versus days in subcultures, started from passages 1–20 (P_{1-20}).
(B) Real-time RT-PCR of activated NEMPs (P_3) and their differentiated progeny (P_{11}), compared with BMMCs. Values represent mean ± SEM (n = 4 for P_3, n = 6 for P_{11}, * $P < 0.05$, ** $P < 0.01$, *** $P < 0.001$). PriCells: Primary muscle cells cultured for five days.
(C) Diagram summarizes different levels of transcripts from Figure 1B, showing *nestin*[hi]*MyoD*[hi]*myogenin*[hi] and *Pax3* in NEMP-P_3 and *MyoD*[hi]*Myf5*^{hi}*Pax3*^{hi} in NEMP-P_{11}, but more uniform transcripts in BMMC-P_3 and -P_{11}.

Analysis of additional neural progenitor markers by immunocytochemistry revealed that Musashi 1 (Msi1) and glial fibrillary acidic protein (GFAP) were expressed in 98.7% and 50.4% of NEMPs (P_{5-6}), but were weakly (84.9%) or negatively detected in BMMCs (Fig. 2A). Thus, the majority of $MyoD^+$ cells (19.3%) in NEMPs co-expressed Msi1 at this stage; in contrast, 37.4% of BMMCs co-expressed MyoD and low levels of Msi1 (Fig. 2A). In P_{8-12}, 41.6% of NEMPs expressed MyoD, but only 9.6% of $MyoD^+$ cells were detected in P_{16-20} (Fig. 2B). However, 85.4–95.3% of BMMCs expressed MyoD and Pax7 in P_{8-12}, and maintained at 42.7–57.8% in P_{16-20}. By flow cytometry, both populations expressed stem cell markers ABCG2 and Sca-1, but CD34 (27.9%) and CD24 (60.1%) were detected in BMMCs (Fig. 2B), which are markers for hematopoietic progenitors, and also are expressed in non-blood cells [32]. The results further supported that early NEMPs exhibited phenotypes for neural/muscle progenitors (*nestin*[hi]Msi1^{hi}GFAP[+]*MyoD*[hi]). By contrast, while the marker profiles suggest the multipotency of BMMCs, the cells could

produce adult-like myoblasts ($MyoD^+Pax7^+$) for more than 50 population doublings.

Markers	GFAP	Msi1	Wnt-1	Pax3	MyoD	Nanog
NEMPs (P5/6)	++	++++	++++	+	+	-
BMMCs (P5/6)	-	(+++)	(+++)	-	++	-

B

Markers	NEMPs		BMMCs	
	P8-12	P16-20	P8-12	P16-20
* Desmin	++++	+	++++	+++
MyoD	++	+	+++	++
Pax7	(++)	-	++++	+++
Myogenin	-	-	+	-
** ABCG2	+++	ND	++	ND
Sca-1	+	++	+	++
CD133	-	-	-	-
CD34	-	-	++	-
CD24	-	ND	+++	++

Figure 2. *Analysis of Marker Profiles by Immunocytochemistry and Flow Cytometry.*

(A) Immunostaining of neural progenitor markers shows positive/high expression of GFAP and Msi1 in NEMP-P$_6$, and negative/low expression of these markers in BMMCs. Arrowheads indicate MyoD$^+$/Msi1^{hi} cells in NEMPs, and MyoD$^+$/Msi1^{low} cells in BMMCs. Note that Msi1 was localized in nuclei and cytoplasm.
(B) Immunocytochemistry (*) and flow cytometry (**) of P$_{8-12}$ and P$_{16-20}$. The percentage of positive cells in (A) and (B) was: −, < 5%; +, 5–25%; ++, 26–50%; +++, 51–90%; ++++, > 90%. The values in parentheses indicate the weakly stained cells.
Scale bars, 20 µm in A.

3.2. NEMPs, but Not BMMCs, Underwent Initial Neuromuscular Differentiation and Produced Embryonic-Like Myotubes in Culture

A distinct feature of the early NEMPs was their spontaneous differentiation into spindle-shaped mosaic myotubes (SMMts), some of which resulted from radial glia-like cells and myoblasts (Fig. 3A). The initial generation of SMMts did not require common differentiation conditions (2% serum), and is agreement with high expression of *MyoD* and *myogenin* transcripts of the cells. Immunocytochemistry revealed that SMMts expressed glial marker S-100, neuron-specific beta-III tubulin, and early myogenic cell marker desmin (Fig. 3A). They were also positive for radial glial marker GFAP, and a few of them (0.7%) became organized into a tissue pattern (Fig. 3B). Approximately half of the SMMts expressed neural markers beta-III tubulin, GFAP, and S-100, and 93% of them expressed desmin, supporting their myotube phenotype (Fig. 3C). In comparison, the majority of BMMCs did not fuse in the growth medium (Fig. 3D), although occasional cells expressed S-100 (4%) and beta-III tubulin (3%). One of the characteristics of BMMCs was their ability to form desmin$^+$ colonies with myoblasts. Quantitative analysis indicated that only 0.6% of BMMCs formed myotubes, while 15.3% of NEMP cells could generate SMMts following initial differentiation (Fig. 3E).
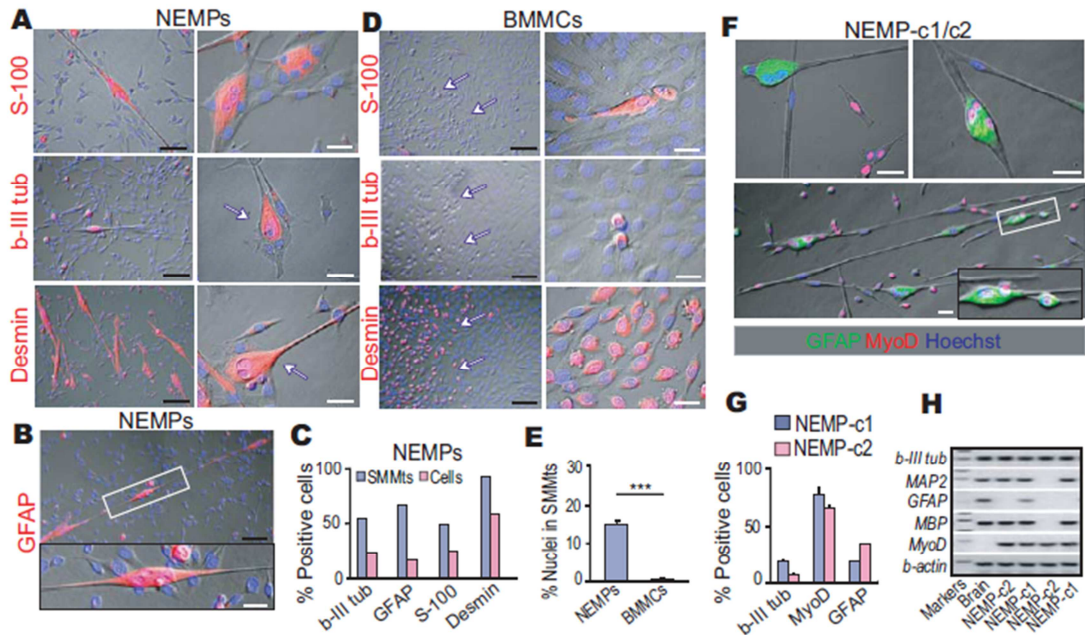

Figure 3. *NEMPs, but Not BMMCs, Underwent Initial Neuromuscular Differentiation.*

(A, B) Differential interference contrast (DIC) images merged with immunostaining show that radial glia-like cells (arrows) and SMMts expressed neural and myogenic markers in NEMP cultures.
(C) For each staining, 55–84 SMMts and 1130–1550 cells were counted.
(D) BMMCs generated S-100$^−$/beta-III tubulin$^−$/desmin$^+$ colonies (arrows).
(E) Percentage of cells fused into SMMts (mean ± SEM, *n* = 5 to 6 cultures, *** *P* < 0.001).
(F, G) NEMP-c1 and −c2 cells differentiated into GFAP$^+$ radial glia-like cells, GFAP$^+$MyoD$^+$ cells, and SMMts. Quantitative analysis was carried out from two to three separate cultures.
(H) RT-PCR was performed with two samples from each cell type, confirming the neuromuscular phenotypes of SMMts. B-III tub and b-actin: beta-III tubulin and beta-actin.
White scale bars, 25 µm; black scale bars, 100 µm.

Similar to NEMPs, NEMP-c1 and -c2 also differentiated into GFAP[+] radial glia-like cells, MyoD[+]GFAP^{+} cells, and SMMts (Fig. 3F and 3G). RT-PCR confirmed the presence of *beta-III tubulin*, microtubule-associated protein 2 (*MAP2*, a neuronal marker), myelin basic protein (*MBP*, an oligodendrocyte marker) and *MyoD* mRNAs in NEMP-c1 and -c2 cultures, as well as *GFAP* in NEMP-c1 (Fig. 3H). The SMMts resembled embryonic myotubes that formed in culture [33–35]; however, the neural commitment of NEMP cells to myotubes suggests a novel myogenic pathway.

3.3. Long-Term Myotube Formation of BMMCs Versus Limited Myogenic Potential of NEMPs in Culture

In the growth medium, NEMP's early progeny rapidly lost their ability to fuse into SMMts. However, the NEMPs at P_{8-12} could undergo secondary myofiber formation in the differentiation medium, leading to many long and multinucleated myotubes (Fig. 4A), like the fetal myofibers [33–35]. By contrast, BMMCs maintained myotube formation from P_8 to P_{20} (Fig. 4A). NEMP-c1/c2 could also generate multinucleated myotubes during differentiation (Fig.

4B). The percentage of cells fused into myotubes was 81.8% in P_{8-12} and 5.2% in P_{16-20} of NEMPs, and 70.2% in P_{8-12} and 48.4% in P_{16-20} of BMMCs (Fig. 4C). The population doubling time of BMMCs was significantly shorter than that of NEMPs and NEMP-c1 (Fig. 4D). Thus, under the same culture conditions, BMMCs frequently produced more myotubes than NEMPs. To confirm the myotube phenotype, we examined myosin heavy chain (MyHC) isoforms and observed muscle-specific proteins MyHC-I and MyHC-embryonic isoforms in BMMC- and NEMP-related myotubes (Fig. 4E).

We further investigated the nature of NEMP-P_{20} after 5-day differentiation in the low serum medium. By skeletal myosin immunostaining, we observed well-developed SMMts consisted of multinucleated myotubes several millimeters in length in the cultures (Fig. 4F). By scanning three entire 60-mm culture wells, three tissue-like SMMts expressing myosin were observed. The unique structure of these SMMts provided important evidence for a potential physiological role of NEMP's initial neuromuscular differentiation (Fig. 4G).
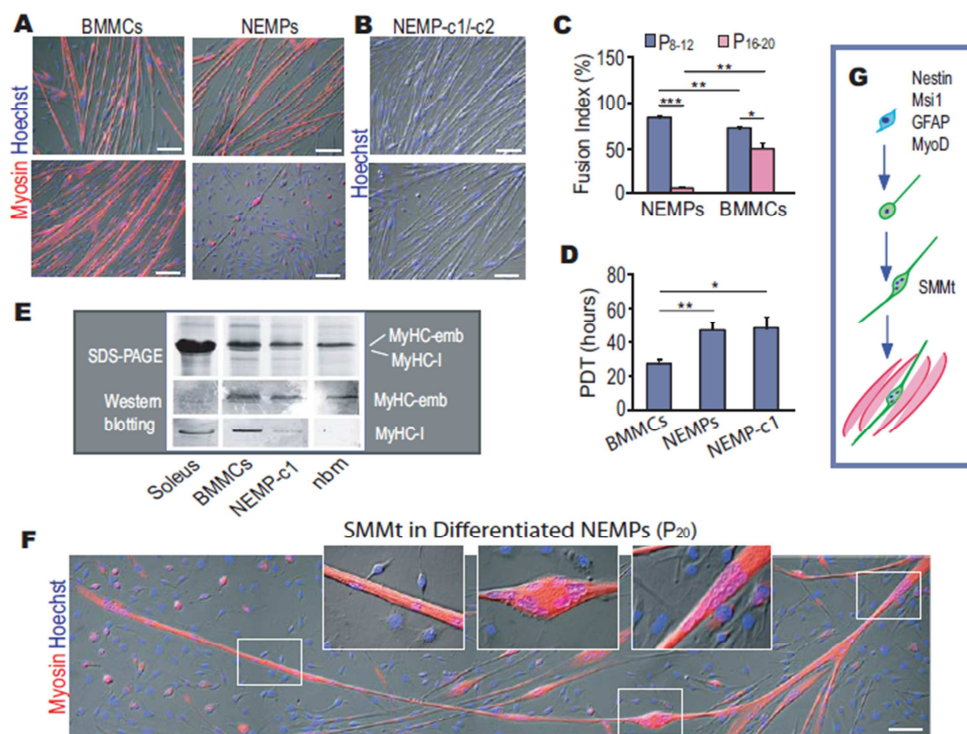

Figure 4. In Vitro Myotube Formation of NEMPs and BMMCs.

(A) Many long and multinucleated myotubes were generated by BMMC- and NEMP-P_{8-12} (upper panels), and also BMMC- but not NEMP-P_{16-20} (lower panels).
(B) NEMP-c1 (upper) and -c2 (lower) could also generate myotubes.
(C) Fusion index was expressed by the percentage of nuclei in myotubes to total nuclei. Values represent mean ± SEM ($n = 5$ to 6 individual trials, * $P < 0.05$, ** $P < 0.01$, *** $P < 0.001$).
(D) Population doubling time (PDT) was analyzed in P_{8-12} (mean ± SEM, $n = 8$ cultures, * $P < 0.05$, ** $P < 0.01$).
(E) MyHC isoforms were identified in myotubes from P_{8-12}. The adult soleus muscle and newborn muscle (nbm) were used as positive controls for MyHC-I (in soleus) and MyHC-embryonic bands (in nbm).
(F) A well-developed SMMt was present in differentiated NEMPs.
(G) Scheme shows the generation of SMMt and its hypothetical role in early muscle formation.
Scale bars, 100 μm in A, B and F.

3.4. NEMPs and BMMCs Restored Dystrophin Expression but NEMPs Produced Embryonic/Fetal-Like Myofibers in Dystrophic Muscles

To examine the transplantation capacity of the cells, we grafted NEMPs, NEMP-c1 and BMMCs into the gastrocnemius muscles of dystrophin-deficient *mdx* mice, an animal model for DMD. Cells at P_{8-12} were used due to their proliferation and myotube formation in vitro. Numerous dystrophin$^+$ fibers were detected in the 14-day grafts of NEMPs and BMMCs (Fig. 5A), and also observed heterogeneously (3:10) in 40–50-day NEMP (Fig. 5B) and NEMP-c1 grafts (not shown). Notably, two types of NENP grafts were identified by distinct donor myofibers (Fig. 5A): being large and centrally nucleated (CNFs), or tiny and peripherally nucleated (PNFs). These myofibers resembled the skeletal muscle that formed during embryogenesis [35, 36], which is correlated with the phenotype of grafted cells ($Pax3^{hi}MyoD^{hi}Myf5^{hi}$). By contrast, the early grafts of BMMCs consisted of more homogeneous dystrophin$^+$ CNFs (Fig. 5A). Given the high percentage of Pax7$^+$MyoD$^+$ cells grafted, the central nucleation of BMMC fibers fits the characteristic of regenerating fibers developed from postnatal muscle precursors [37]. Interestingly, although the majority of BMMC myofibers were lost in eight late grafts of mdx mice (Fig. 5C), more than 800 healthy dystrophin$^+$ fibers were generated 35 days after grafting a small number of BMMCs (5×10^4) into irradiated muscles of *mdx* nu/nu mice (Fig. 5D). The irradiation has been reported to inhibit endogenous myoblast activation, thus improving the long-term survival of donor myofibers [38].

Quantitative analysis revealed that the number of dystrophin$^+$ fibers was high in the 14-day grafts of BMMCs and NEMPs, and decreased dramatically by 87% and 77% in 40–50-day grafts, but remained higher in grafted sites than non-grafted sites (Fig. 5E). The percentage of dystrophin$^+$ CNFs in NEMP grafts was lower than that in the BMMC grafts (Fig. 5F). The dystrophin$^+$ fibers of NEMP-c1 were smaller than the fibers in non-grafted sites (Fig. 5G). Generally, BMMCs produced homogeneous dystrophin$^+$ fibers in early grafts in terms of the percentage of CNFs (average 33.7%, ranged 30.1%–36.0%) and the relative diameter of fibers (average 18.0 μm, ranged 17.6–18.6 μm). By contrast, the grafts of NEMPs and NEMP-c1 were largely heterogeneous with regard to the number, nuclear location, and diameter of donor fibers. We observed ten grafts from 13 NEMP-injected muscles. Of these grafts, six had a low percentage of CNFs (average 11.9%, ranged 9.9%–17.1%), five of which were correlated with the small diameter of fibers (average 13.3 μm). Four grafts had a higher percentage of CNFs (average 41.1%, ranged 34.7%–47.7%), three of which were correlated with the large diameter of myofibers (average 28.5 μm). In summary, NEMPs generated two major types of grafts resembling enlarged embryonic and fetal myofibers, which are distinct from the regenerating fibers of BMMCs (Fig. 5H).

Next, we analyzed the histological features of six late grafts that exhibited large numbers of dystrophin$^-$ fibers in the grafted sites (Fig. 5I). In the area, the percentage of dystrophin$^-$ PNFs was higher in NEMP/NEMP-c1 grafts than in BMMC grafts (Fig. 5J). In the NEMP/NEMP-c1-grafted sites, there were numerous small, rounded, regenerating PNFs, and increased endomysial tissue (Fig. 5I). These resembled the histopathological features of skeletal muscle disease, and were distinct from the satellite cell-regenerated CNFs (Fig. 5I). The presence of disease-like tissues provides an explanation for the loss of NEMP-derived dystrophin$^+$ fibers in some of the late grafts.

3.5. Maturation Analysis of Dystrophin$^+$ Fibers Associated with MyHC Expression and Muscle Satellite Cells

To track the maturation of donor-related myofibers, we further examined the expression of developmental MyHC in the grafted muscles. The MyHC was detected in approximately 70% of dystrophin$^+$ fibers in the 14-day grafts of NEMPs, but was < 1% in the 40–50-day grafts of NEMPs and NEMP-c1 (Fig. 6A and 6C). The results suggest that maturation of NEMP myofibers in host muscle had occurred. Interestingly, > 99% of BMMC fibers did not express development MyHC in the 14- and 40–50-day grafts (Fig. 6B and 6C). The findings indicated that the majority of NEMP fibers were homogeneous in donor origin, while the dominant dystrophin$^+$ fibers in BMMC grafts were heterotypic, a result from fusion of donor cells with host fibers or myoblasts [39].

We then examined whether adult muscle progenitors existed in the grafts. Following transplantation, Pax7$^+$ cells were detected in BMMC, NEMP and NEMP-c1 grafts (Fig. 6D). In the early grafts, the number of Pax7$^+$ cells in NEMP-grafted sites was 2.8-fold greater than that in BMMC-grafted sites (Fig. 6F). Analysis of MyoD, which is expressed in activated but not quiescent adult myoblasts [40,41], showed that no differences were observed between Pax7$^+$ and MyoD$^+$ cells in BMMC grafts, while Pax7$^+$ cells were 3.3-fold greater than MyoD$^+$ cells in NEMP grafts. Consistent with the phenotype, large numbers of donor fibers in NEMP grafts remained small and peripherally nucleated, which did not support an adult myoblast function of the Pax7$^+$ cells, because satellite cell-mediated muscle regeneration in adults will result in the fuse of cells into CNFs [37, 42]. Notably, in the most significant late graft of NEMPs with more than 800 donor myofibers, 10.6% of CNFs, and myofiber diameter of 21.5 μm, we were unable to detect clear Pax7$^+$ satellite cells (Fig. 6E). Thus, growth of these myofibers is independent of the Pax7$^+$ cells observed in the early NEMP grafts. Together, the results indicate that BMMCs function as more committed muscle precursors, but the NEMP myofibers encounter impaired maturation with a defective adult fate in vivo, as characterized by the presence of non-fusing Pax7$^+$ cells or the lack of satellite cells in grafts.
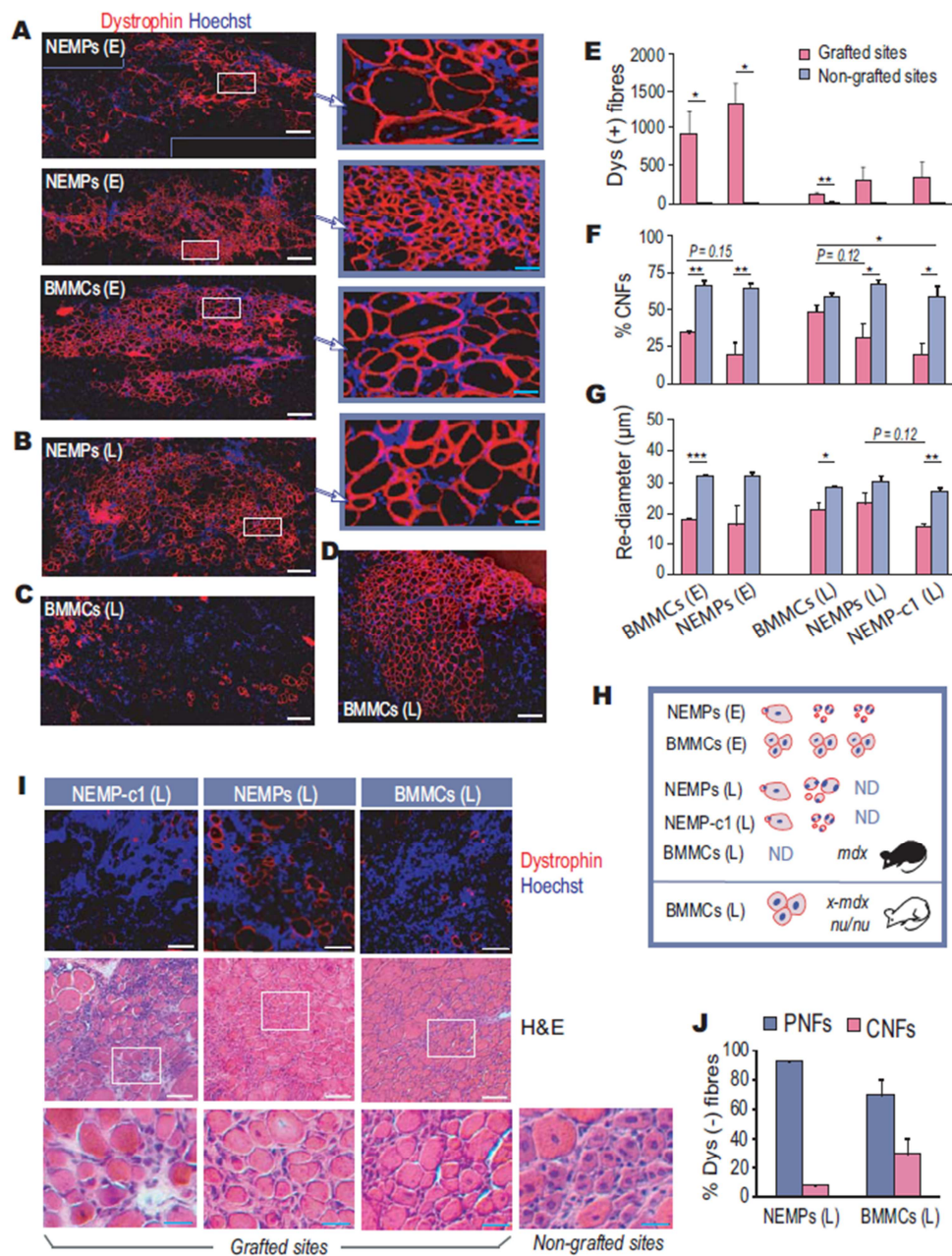
Figure 5. *NEMPs and BMMCs Generated Distinct Myofibers in Dystrophic Mice.*

(A) Dystrophin[+] fibers in three early grafts (E). The box areas in the left panels were magnified in the right panels showing large CNFs (upper) or small PNFs (middle) in NEMPs, and more uniform CNFs in BMMCs (lower).

(B) Many PNFs were present in one of the NEMP's late grafts.

(C) Dystrophin[+] fibers decreased dramatically in BMMC late grafts.

(D) BMMCs generated large late grafts in irradiated *mdx* nu/nu mice.

(E–G) Quantitative analysis of dystrophin[+] (dys[+]) fibers in mdx mice (mean ± SEM, n = 3, 3, 8, 5 and 5 muscles in E, and n = 3–6 muscles in F and G, * $P \leq$ 0.05, ** $P < 0.01$, *** $P < 0.001$). The number of dys[+] fibers has been normalized to the number of injected cells in E (3×10^5 cells). The muscles with low numbers of dys[+] fibers are not shown in F and G: in this case, the data were impossible to interpret due to the presence of revertant fibers from spontaneous mutations [59]. Re-diameter: Relative diameter.

(H) Scheme summarizes two types of NEMP grafts with embryonic- or fetal-like myofibers, and homogeneous BMMC grafts with regenerating fibers. ND: No grafts with large clusters of dys[+] fibers (> 50 fibers) were detected.

(I) Serial sections of three muscles show disorganized dystrophin[−] PNFs and increased interstitial tissues in NEMP-grafted sites, histopathologically distinct from satellite cell-regenerated CNFs in non-grafted sites.

(J) The percentage of dys[−]-PNFs and dys[−]-CNFs in grafted sites (mean ± SEM, n = 3 muscles).

White scale bars, 150 μm in A–D; 75 μm in I; Blue scale bars, 25 μm in A, B and I.
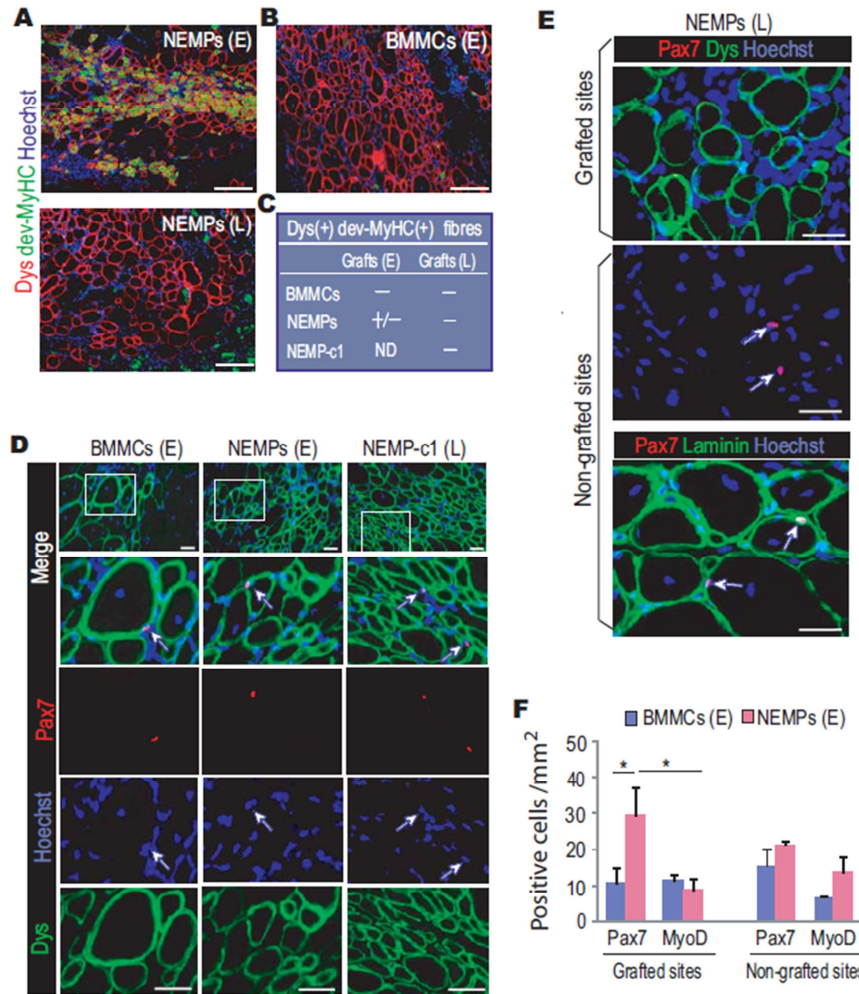
Figure 6. *Differential Maturation of Dystrophin⁺ Fibers from NEMPs and BMMCs.*

(A, B) Dystrophin (dys) and developmental MyHC (dev-MyHC) double immunostaining of the early (E) and late grafts (L).

(C) Dev-MyHC$^+$ myofibers per 100 dys$^+$ fibers: −, 0−0.2%; +/−, 71.5%. Each value represents the mean of three muscles. ND: Not determined.

(D) Pax7$^+$ cells (arrows) in CNFs (left panels) or small PNFs (middle and right panels).

(E) Same muscle section of a late NEMP graft shows no Pax7$^+$ cells in grafted sites, and Pax7$^+$ cells (arrows) in non-grafted sites, where CNFs were revealed by laminin staining in a serial section.

(F) Histogram shows no differences between Pax7$^+$ and MyoD$^+$ cells in BMMC-grafted sites, but higher Pax7$^+$ cells than MyoD$^+$ cells in NEMP-grafted sites (mean ± SEM, n = 3 muscles, * $P < 0.05$).

Scale bars, 100 μm in A and B; 25 μm in D and E.

3.6. Multi-Lineage Neural Differentiation of NEMPs Versus Limited Neural Potential of BMMCs

Based on the initial neuromuscular differentiation of NEMPs, we then investigated the neurogenic potential of NEMP-P$_{8-12}$, compared with BMMCs. In standard culture conditions, we observed higher levels of neuronal transcripts beta-III tubulin and MAP2 in NEMPs and NEMP-c1, and a high level of NG2 (a marker for oligodendrocytes and pericytes) in BMMCs (Fig. 7A). When cultured in the neurosphere formation and differentiation conditions supplemented with brain-derived neurotrophic factor, MAP2$^+$ and beta-III tubulin/Tuj1$^+$ cells were observed in all the populations, some of which had typical neuronal morphology, especially in the NEMP-c1 (Fig. 7B and 7C). Very few of BMMCs showed the morphology of neurons.

Thus, the generation of neurons in NEMP populations correlates with their higher expression of neuronal transcripts in the untreated cells. RT-PCR confirmed the expression of lineage markers for neurons and oligodendrocytes in the treated NEMP cells and BMMCs (Fig. 7D). In particular, astrocyte marker *GFAP* was detected in both treated and untreated NEMPs. The findings demonstrate multi-lineage neural differentiation of NEMP-P$_{8-12}$. However, given the defective adult fate for the myogenic lineage, it remains unknown whether mature neurons could be established from the embryonic-like progenitors.

Next, we developed NEMP clones by seeding single cells into the 96-well plates. After isolation and expansion for a short period, analysis of two clones revealed that clone 1 displayed low levels of Msi1, high levels of NSE (neuron-specific enolase), and 31.6% of MyoD$^+$ cells, while the clone

2 showed high levels of Msi1, low levels of NSE, and only 1.1% of MyoD$^+$ cells (Fig. 7E). Thus, single cells from NEMPs differentiated into neural and muscle cells.

Due to the glial differentiation in vitro, we tracked NEMP-c1 in four grafted muscles of female mice by FISH analysis, and detected Y-chromosome$^+$ cells at a low frequency in the peripheral nerves (6.88 ± 0.43, mean ± SEM, n = 4 muscle samples; 0, n = 3 control samples, average of 15 sections per sample). Immunostaining revealed some Y-chromosome$^+$ cells relevant to GFAP-expressing glial cells (Fig. 7F).
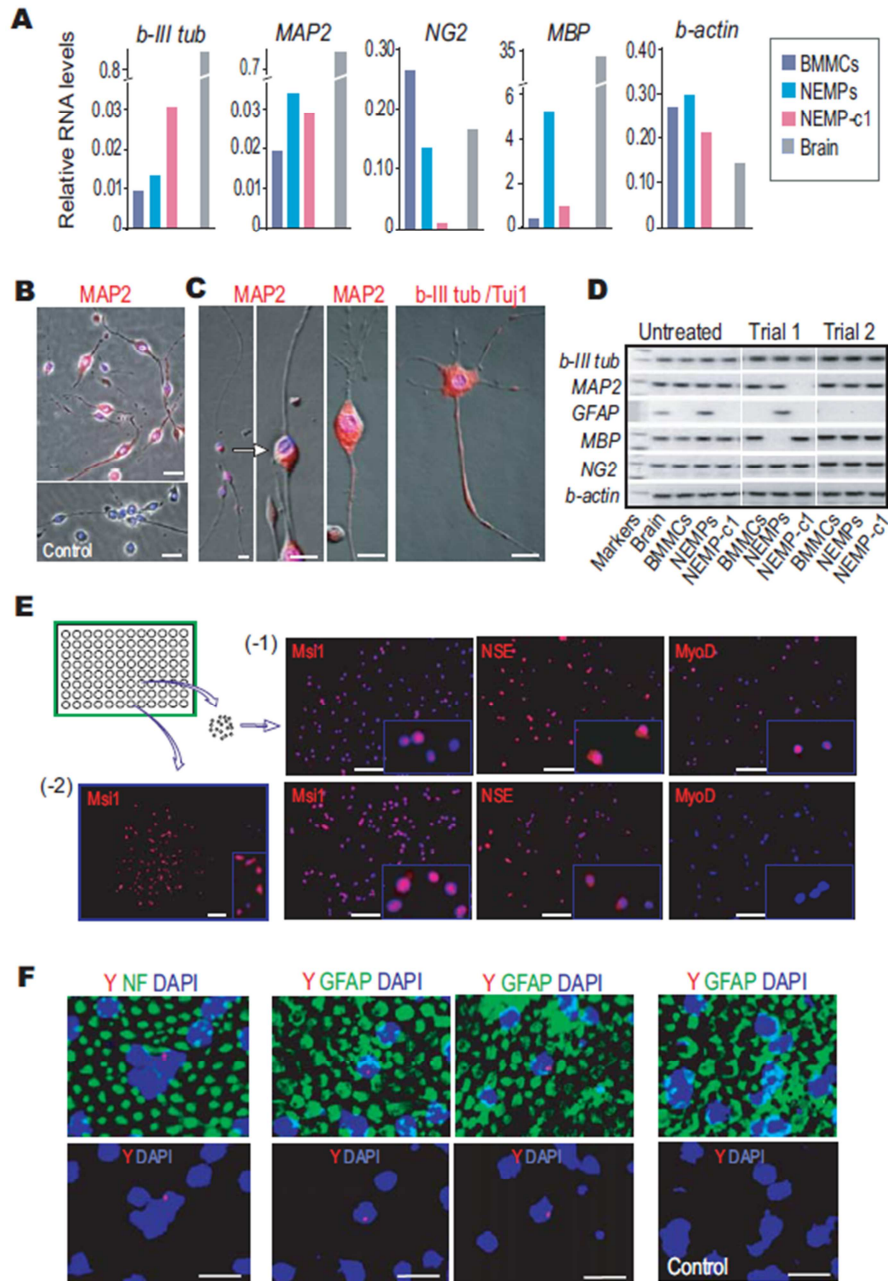

Figure 7. Multi-Lineage Neural Differentiation of NEMPs versus Limited Neural Potential of BMMCs.

(A) Quantitative RT-PCR was performed with untreated cells in two samples from each cell type, showing higher levels of *beta-III tubulin* and *MAP2* in NEMP cells and higher *NG2* in BMMCs.

(B, C) Cells were treated by neurosphere formation and differentiation, and expressed neuronal markers in the cultures of NEMP-c1.

(D) Transcripts were measured by RT-PCR and adult brain tissues were used as the positive control. Both untreated and treated cells expressed identical mRNAs with the exception that MAP2 and MBP were not detected in the treated NEMP-c1 or NEMPs in Trial 1, but were expressed in Trial 2 when laminin was added into the neurobasal medium. GFAP was only detected in NEMPs.

(E) Two single clones were established from cultured NEMPs, and analyzed for the expression of Msi1, NSE and MyoD. Note that clone 2 (-2) generated a new clone (Msi1^{hi}, lower left panel) during expansion. Nuclei were stained by Hoechst.

(F) Y chromosomes were detected in peripheral nerves of NEMP-c1-grafted muscles. NF: Neurofilament.

Scale bars, 25 μm in B; 15 μm in C and F; 100 μm in E.

4. Discussion

In the present study, we have demonstrated two new types of multipotent myogenic progenitors from adult skeletal muscle and bone marrow. The differentiation of NEMPs into radial glial and embryonic/fetal myoblast lineages has been the first report by using muscle cell isolations. In addition, the isolation of myogenic cells from bone marrow supports previous observations [5, 7], but also provides additional evidence for a distinct subset of bone marrow, capable of generating muscle cells for more than 50 population doublings. The original NEMPs are considered to be one cell per 130 mg mouse muscle. The rarity and lack of a physiological role to postnatal muscle tissue suggest the potential identity of NEMPs as embryonic remnants. This character distinguish NEMPs from subpopulations of muscle satellite cells [16–18, 43], or muscle-derived pericytes and interstitial progenitors [44–46], which are relative abundance in tissue (hundreds or thousands of sorted cells per 100 mg muscle), and functionally related to postnatal muscle, vasculature or connective tissues. However, whether NEMPs exist in some of the muscle-based cell cultures is unknown, and their potential impact on the biological behaviors of these cells needs to be established. Notably, the vascular-related progenitors (pericytes or mesoangioblasts) have been presumed to represent embryonic cells present in the postnatal tissue [44]. It might be interesting to examine whether the multi-lineage differentiation of such cells is related to an embryonic fate.

In a previous report, a small population of CD34^{+}/Sca-1^{+} progenitors was isolated from muscle of newborns, which exhibited extensive proliferation as myogenic cells for 30 passages [6]. Interestingly, we did not find a similar population in adult skeletal muscle, despite analyzing multiple primary colonies from 5-, 7- and 10-week-old mice. A reasonable explanation for this discrepancy is that the CD34^{+}/Sca-1^{+} cells represent a distinct high-proliferating myogenic population in newborn muscles [47, 48], which may overgrow to replace the slow-dividing NEMPs when the initial culture contains both cell types.

The distinct myogenic fates of NEMPs and BMMCs suggest that their differentiation in vitro might mimic distinctive stages in muscle development. During limb myogenesis, Pax3^{+} muscle progenitors differentiate into MyoD and Myf5-expressing embryonic and fetal myoblasts that form different stages of skeletal muscle in embryos [29–31]. At postnatal stage, quiescent adult myoblasts/satellite cells expressed Pax7 [49], and also MyoD and/or Myf5 when activated, to produce regenerating myofibers [40, 41]. Compared to this model, early activated BMMCs expressed a higher level of Myf5 and produced Pax7^{+}MyoD[+] adult myoblasts for more than 50 population doublings. By contrast, NEMPs generated two waves of myogenic cells by a temporal manner: initial up-regulation of Pax3 in early passages and a higher level of MyoD/Myf5 in late passages, similar to embryonic and fetal myogenic pathways. The different expression patterns of myogenic markers in NEMPs and BMMCs were further confirmed by their respective generation of distinct myotubes/myofibers in culture and in transplants. The findings demonstrate that after activation in vitro, the NEMPs function as embryonic muscle progenitors, while the BMMCs serve as postnatal myogenic precursors (Fig. 8).

Neurogenic conversion of muscle-derived cells has been examined [50, 51]; the present study, however, was designed to characterize a novel type of neurogenic/myogenic progenitors from skeletal muscle. The activated NEMP cells expressed high levels of neural progenitor markers nestin, Msi1 and GFAP [28, 32], and could generate radial glia and neurons in culture. Radial glial cells normally arise from the embryonic neuroepithelium and function to guide migration of immature neurons [52]. Our findings, therefore, support the NEMPs as embryonic neural progenitors present in postnatal skeletal muscle. The co-expression of MyoD and GFAP in the activated single NEMPs and their spontaneous differentiation into radial glia-associated myotubes/SMMts demonstrate a unique progenitor for both neuroepithelial and myogenic lineages. Although similar progenitors have not been reported previously, the co-presence of cells with muscle, glial and neuronal phenotypes in rhabdomyosarcoma [23] suggests the existence of such progenitors in postnatal muscle. In the present study, we did not explore the potential location of NEMPs in tissue. Based on the generation of SMMts, we hypothesize a possible source of NEMPs in association with a small number of neuromuscular spindles, the stretch receptor organs within skeletal muscle.

Transplantation experiments demonstrated distinct roles of NEMPs and BMMCs in muscle regeneration. The BMMCs established healthy engraftments in *mdx* (early grafts) and irradiated *mdx nu/nu* mice, the latter showing one of the best engraftments with this animal model [16]. Because one BMMC can produce at least 10^9 muscle cells, it provides efficient myogenic precursors in cell replacement strategy. The generation of large numbers of dystrophin[+] myofibers by BMMCs also demonstrates the in vivo muscle differentiation of marrow-derived cells [5, 7] rather than a simply non-myogenic fusion. By contrast, the NEMP cells produced unusual grafts with embryonic/fetal-like dystrophin[+] myofibers that could, to some extent, adapt to a postnatal differentiation program, leading to the long-term survival of engraftments. However, the presence of Pax7^{+} non-fusing cells or the lack of satellite cells in grafts suggests abnormal or restricted adult fates of NEMPs in vivo, presumably due to their intrinsic differentiation potential and the lack of a normal developmental niche in the dystrophic muscles.

In cell transplantation, mdx mice, which lack dystrophin in the membrane of muscle fibers, were used. Compared with DMD patients, the mdx mice show less severe myopathology, and efficient muscle regeneration, resulting

in more than 50% of CNFs in the adult animals [42, 53]. However, grafting of NEMPs altered the histopathological features of mdx muscle to that similar to DMD patients. First, NEMPs produced fetal-like myofibers or regenerating myofibers with a low percentage of CNFs, which has only been reported in patients with DMD [54], and in the extensively damaged diaphragm of mdx mice [55]. Second, the fetal-like grafts lacking satellite cells or showing increased number of non-fusing Pax7+ cells is in agreement with the features of satellite cell deficiency [56], or the presence of defective satellite cells in DMD patients [57, 58]. Third, dystrophin− fetal-like fibers existed in grafted sites. The recapitulation of DMD patient's muscle tissue suggests that activated primitive NEMPs and their early myogenic progeny are potentially associated with DMD pathogenesis, and should be excluded in cell transplantation for repair of muscle damage in this myopathy.

In conclusion, we have demonstrated that embryonic-like neural/muscle progenitors can be isolated from adult skeletal muscle, and differentiate in vivo into fetal-like muscles recapitulating myofiber and satellite cell abnormalities of DMD patients, thus representing a potential cellular origin of diseased tissues. In parallel studies, bone marrow-derived progenitors contribute to adult muscle precursors capable of repairing dystrophic mice. Identification of the two types of embryonic- and adult-like progenitors may have different implications in cell replacement strategy, and enhance our understanding the etiology and progression of relevant human diseases. Based on the embryonic fate and lack of physiological roles, we suggest that the adult-origin NEMPs may provide a unique disease-associated cell type for therapeutic development.
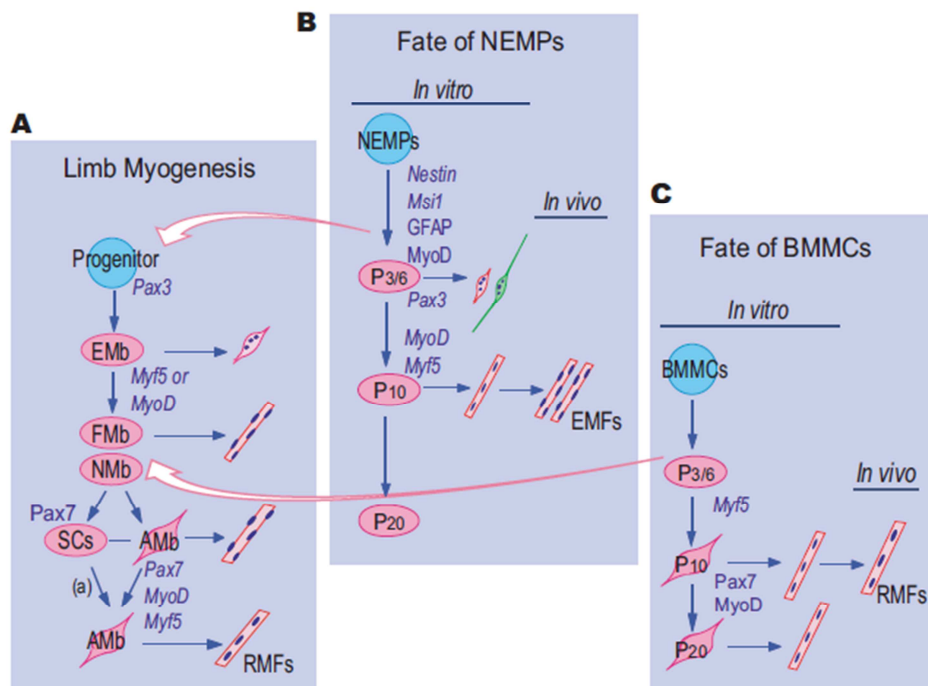

Figure 8. *The Differentiation Hierarchy and Cell Fate of NEMPs and BMMCs Compared with Limb Myogenesis.*

(A) During myogenesis, muscle progenitors (Pax3+) differentiate into embryonic (EMb), fetal (FMb), and neonatal/adult myoblasts (NMb/AMb), which generate different stages of skeletal muscles. In adults, quiescent satellite cells (SCs) express Pax7, and also MyoD and Myf5 when activated (a), to produce regenerating myofibers (RMFs).
(B) The activated NEMPs express neuroepithelial and myogenic progenitor markers, and differentiate into early myoblasts that form embryonic/fetal-like myofibers (EMFs) in vivo.
(C) BMMCs can differentiate into adult-like myoblasts (Pax7+/MyoD+) that regenerate dystrophic muscles. Large arrows indicate the NEMP and BMMC hierarchy in association with limb myogenesis.

Abbreviations

BMMCs, bone marrow myogenic cells; CNFs & PNFs, centrally or peripherally nucleated fibers; MyHC, myosin heavy chain; DMD, Duchenne muscular dystrophy; GFAP, glial fibrillary acidic protein; MAP2, microtubule-associated protein 2; MBP, myelin basic protein; NEMPs, neuroepithelial myogenic progenitors; SMMts, spindle-shaped mosaic myotubes

Supplementary Information (Experimental Procedures)

1. Animals

Normal C57BL/6 mice, and *mdx* mice (C57BL/10ScSn-Dmd^{mdx}/J, purchased from Jackson Laboratories, USA) were used in this study. The mice were maintained in the Animal Facilities of the Panum Institute, University of Copenhagen

and the animal protocols were approved by the Animal Care and Ethics Committee in Copenhagen.

2. Cell Isolation

NEMPs were isolated from skeletal muscle of C57BL/6 mice (five weeks old). Briefly, the hindlimb muscles were digested by 0.2% collagenase-type XI (Sigma-Aldrich) at 37°C for 1 h, 0.25% dispase for 45 min, and 0.1% trypsin-EDTA for 30 min. The cells were then filtered through a 70-μm nylon mesh (BD Biosciences) and centrifuged at 3 500 r/min for 5 min. The pellets were resuspended in the growth medium, and the cells were plated onto 0.01% collagen type 1-coated flasks (BD Biosciences) and cultured in a humidified incubator at 37°C with 5% CO_2. The growth medium consisted of DMEM supplemented with 10% horse serum, 10% fetal bovine serum, 0.5% chick embryo extract (Sera Laboratory International), and 1% penicillin-streptomycin (all reagents were purchased from Life Technologies unless stated otherwise). The primitive NEMPs took 5–6 days to attach to culture flasks, and thus they can be separated by preplate from the majority of cells that attached during the first 4 days [6, 25, 26]. On day 5, the floating cells were collected and centrifuged. The pellets were resuspended in the growth medium and seeded onto 12-well dishes at ~15–30 cells/cm^2 to develop NEMP clones from primary cultures. During the following 2 weeks, the medium were changed daily and the initial NEMP colonies with 50–100 cells were formed. The early NEMP cells were small round or spindle-shaped, and phase-bright. To confirm the clonal property, the primary colonies were picked up, and seeded in new 12-well dishes at the clonal density. When new colonies were formed within another two weeks, the wells containing single colonies were chosen as the primary NEMP clones. Colony cylinders (Sigma-Aldrich) were used to select primary colonies or purified clones.

To isolate BMMCs, the femurs of C57BL/6 mice (seven weeks old) were removed, and the bone marrow was flushed out with HBSS using a 25-gauge needle. The bone marrow samples were centrifuged at 3 500 r/min for 5 min, and the cells were collected and incubated with muscle extract for 30 min. To prepare the muscle extract, 300 mg of hindlimb muscle of normal mice was minced and incubated in 5 ml of 0.2% collagenase-type XI (Sigma-Aldrich) at 37°C for one hour, and then centrifuged at 3 500 r/min for 5 min. The supernatant (collagenase-muscle extract) was collected and filtered through 0.2–0.4 μm pores to avoid muscle cell contamination. We checked the filtered muscle extract and did not find cells in it. Although we do not know the precise function of the muscle extract, in a pilot study, no myogenic-like cells were present in cultures when marrow cells were not treated with muscle extract, suggesting its potential role for inducing muscle differentiation of bone marrow. After incubation with muscle extract, the bone marrow cells were centrifuged, and resuspended in the growth medium. The cells were cultured in a collagen-coated flask, and further separated by preplate and clonal isolation as described for NEMPs.

3. Neural Differentiation

The neurosphere formation and differentiation were performed as described [50], with modification. In brief, cells were cultured in non-coated 6-well plates in neurobasal medium supplemented with 1% penicillin-streptomycin, L-glutamine (2 mM), B27, basic fibroblast growth factor (bFGF, 20 ng/ml), and epidermal growth factor (EGF, 20 ng/ml). Neurospheres were present after 1 day and were grown for 5 days. The cells were then switched to poly-L-lysine-coated plates in neurobasal medium supplemented with N2, EGF (20 ng/ml), bFGF (20 ng/ml), L-glutamine and laminin (1 μg/ml, Sigma-Aldrich) for 1 day. Afterwards, the cells were incubated in neurobasal medium with N2, brain-derived neurotrophic factor (15 ng/ml) and laminin for 2–3 days (all reagents were purchased from Life Technologies unless stated elsewhere). Expression of specific markers for neuronal and glial lineages in the untreated and treated cells was determined by immunocytochemistry, RT-PCR and real-time RT-PCR.

4. Isolation and Analysis of NEMP Clones

NEMPs (P$_{16}$) were plated onto collagen type 1-coated 96-well dishes at a density of 25–50 cells/ml medium, and checked for single cells 1 h after plating. The cells were grown in the growth medium for six days, and single clones were picked up for further expansion. Expression of specific markers for muscle (MyoD) and neural cell lineages (Msi1 and NSE) in two clones was determined by immunocytochemistry.

5. Immunocytochemistry

Cells were fixed in cold methanol for 5–10 min, washed in PBS and blocked in 5% serum or 1% bovine serum albumin for 30 min at room temperature. Primary antibodies used in this study were rabbit anti-desmin (1:100, Sigma-Aldrich), mouse anti-MyoD (1:80, BD Biosciences), mouse anti-myogenin (1:80, BD Biosciences), mouse anti-Pax7 (1:50, R&D Systems), goat anti-Wnt-1 (1:20, R&D Systems), rabbit anti-Msi1 (1:100, Abcam), rabbit anti-Nanog (1:100, Abcam), mouse anti-Pax3 (1:100, R&D Systems), rabbit anti-S-100 (1:300, Sigma-Aldrich), rabbit anti-GFAP (1:200, Sigma-Aldrich), mouse anti-beta-III tubulin (1:300, Millipore), mouse anti-beta-III tubulin/Tuj1 (1:200, R&D Systems), rabbit anti-MAP2 (1:600, Millipore), rabbit anti-NSE (1:100, Sigma-Aldrich), and mouse anti-skeletal myosin fast (1:500, Sigma-Aldrich). Staining was revealed by species-specific Alexa Fluor 594 or 488 (1:500, Life Technologies). The nuclei were revealed by Hoechst 33342 (Sigma-Aldrich). The percentage of positive cells was determined as the ratio of labeled cells to the total number of cells in five randomly chosen fields at 100 × or 200 × magnification. The cells labeled only with secondary antibody, or with irrelevant antibodies were used as negative controls. Fluorescent images were performed using an Olympus IX71 inverted microscope.

6. Flow Cytometry

NEMPs and BMMCs were grown in 75-cm^2 flasks until 15–25% confluence. The cells were then detached with cell scrapers (Sigma-Aldrich) and spun down. Staining was done in PBS containing 1% BSA at 4°C. FITC- or R-PE-conjugated monoclonal antibodies to Sca-1 (BD Pharmingen), CD133 (eBioscience), CD34 (BD Pharmingen), CD24 (Millipore), and Bcrp1/ABCG2 (Millipore) were used. Flow cytometry was performed using EPICS XL-MCL flow cytometer (Coulter) and the percentage of positive cells was assessed by Winlist software.

7. Sodium Dodecyl Sulfate Polyacrylamide Gel Electrophoresis (SDS-PAGE) and Western Blotting

Myosin heavy chain isoform analysis was performed using SDS-PAGE. To determine the MyHC isoform composition in the BMMCs and NEMP-c1 cells, a 10–25 µl pellet obtained from the myotube cultures of each cell population, was dissolved in 150 µl HBSS, mixed with 350 µl Laemmli sample buffer and heated for 4 min at 90°C. Twenty to seventy-five milligrams of muscle from the soleus muscle of adult C57BL/6 mice, and entire legs from newborn C57BL/6 mice, were homogenized in 350–750 µl Laemmli sample buffer and heated for 4 min at 90°C. The myosin-containing samples (8–25 µl) were loaded on an SDS-PAGE gel containing 6% polyacrylamide and 30% glycerol. Gels were run at 4°C at 70 V for 42–44 h. Subsequently, one set of gels was stained with Coomassie Blue to visualize the MyHC bands directly. Another set of gels was blotted onto a PVDF membrane at 500 mA overnight. Membranes were blocked with 5% skimmed milk powder overnight, washed with TBS-T and incubated with the primary antibodies BA-F8 (anti-MyHC-I, 1:100) and BF-G6 (anti-MyHC-embryonic, 1:50) [60] for 2 h at 37°C, washed in TBS-T and incubated in the secondary antibody (1:600, Dako) for 1 h at 37°C, and finally developed with DAD.

8. Real-Time RT-PCR

Total RNA from 5,000–50,000 cells was purified using 150 µl TriReagent (Molecular Research Center) containing 80 µg glycogen. Total RNA (20 ng) was converted into cDNA in 20 µl using the Omniscript reverse transcriptase (Qiagen). For each target mRNA, 0.5 µl cDNA (0.05 µl for *MyoD* and *beta-actin*) was amplified in a 25 µl SYBR Green PCR reaction containing 1×Quantitect master mix (Qiagen) and 100 nM of each primer. The amplification was monitored real-time using the MX3000P Real-time PCR machine (Stratagene). The C_t values were related to a standard curve made with the cloned PCR products or with cDNA dilutions. The quantities were normalized to total RNA (cDNA per ng RNA). For visualization, after PCR to 50 cycles the PCR products were run in 3% agarose gels containing Gelstar (Cambrex). RNA from primary muscle cells, the brain of adult or newborn mice, and 7-day embryos were used as positive controls. The following gene expression assays were performed: *Pax3, Pax7, MyoD, Myf5, myogenin, nestin,*

Sox10, GFAP, beta-III tubulin, beta-actin, MAP2, MBP, NG2 and *Oct-4*. Detailed information for primers is shown in the table below.

Table 1. Primers

Name	Oligo Sequence
Mouse Tubulin-b3 SybrS	TTCGTCTCTAGCCGCGTGAAGT
Mouse Tubulin-b3 SybrA	CATCGCTGATGACCTCCCAGAA
Mouse Sox10 SybrS	ACCACCGGCACCCAGAAGAAG
Mouse Sox10 SybrA	TGGGGTGGTTGGAGGGGTTG
Mouse Pax7 SybrS	TGGCACAGAGGACCAAGCTCAC
Mouse Pax7 SybrA	CCCGGCAGAAGGTGGTTGAAG
Mouse Pax3 SybrS	ACAGACAGCTTTGTGCCTCCATC
Mouse Pax3 SybrA	CGTGGTTGGTCAGAAGTCCCATT
Mouse NG2 SybrS	CCAGCCGTCTCTGGAAGAACAAAG
Mouse NG2 SybrA	TAGGAGGTTGGCGGCATCAAGG
Mouse Nestin SybrS	GCAGCAACTGGCACACCTCAA
Mouse Nestin SybrA	CGAGAGTTCTCAGCCTCCAGCA
Mouse Myogenin SybrS	CAACTCCCACAGCGCCTCCT
Mouse Myogenin SybrA	GTAGGGTCAGCCGCGAGCAA
Mouse MyoD SybrS	CGGCAGAATGGCTACGACACC
Mouse MyoD SybrA	GCTCGACACAGCCGCACTCTT
Mouse myf5 SybrS	CCCGAAAGAACAGCAGCTTTGAC
Mouse myf5 SybrA	GACAAGCAATCCAAGCTGGACAC
Mouse MBP SybrS	ACGGCCGGACCCAAGATGAA
Mouse MBP SybrA	CCCTTGGGATGGAGGTGGTG
Mouse MAP2 SybrS	TAATCTGCCACCTTCGCCACCA
Mouse MAP2 SybrA	GGAGCCTGAGCCAAGTCACCAC
Mouse GFAP SybrS	GGTTGAATCGCTGGAGGAGGAG
Mouse GFAP SybrA	CCACGTGGACCTGCTGTTGG
Mouse bActin SybrS	TGCTGACAGGATGCAGAAGGAGA
Mouse bActin SybrA	CAGAGTACTTGCGCTCAGGAGGA
Mouse Oct-4 SybrS	CGAAGCCCTCCCTACAGCAGA
Mouse Oct-4 SybrA	GGCGCCGGTTACAGAACCATAC

9. In Situ Hybridization

For the detection of the Y-chromosome in NEMP-c1-grafted muscles, a mouse chromosome Y probe (IDMB1055, ID Labs Inc) was used. FISH analysis was carried out according to the manufacturer's instructions, and immunofluorescent staining with neurofilament and GFAP was performed prior to in site hybridization. Sections were fixed in acetone/methanol (1:1) for 10 min at - 20°C, and blocked in 1% BSA for 30 min at room temperature. Sections were then incubated with rabbit anti-neurofilament (1:400, Life Technologies) or rabbit anti-GFAP antibody (1:200, Sigma-Aldrich) for 90 min, FITC-labeled sheep anti-rabbit IgG (1:200, Sigma-Aldrich) for 60 min.

Acknowledgments

References

[1] Weissman, I. L. (2000). Stem cells: units of development, units of regeneration, and units in evolution. Cell *100*, 157–168.

[2] Fuchs, E., and Segre, J. A. (2000). Stem cells: a new lease on life. Cell *100*, 143–155.

[3] Sell, S. (2004). Stem cell handbook. (Humana Press, Totowa).

[4] Salero, E., Blenkinsop, T. A., Corneo, B., Harris, A., Rabin, D., Stern, J. H., and Temple, S. (2012). Adult human RPE can be activated into a multipotent stem cell that produces mesenchymal derivatives. Cell Stem Cell *10*, 88–95.

[5] Gussoni, E., Soneoka, Y., Strickland, C. D., Buzney, E. A., Khan, M. K., Flint, A. F., Kunkel, L. M., and Mulligan, R. C. (1999). Dystrophin expression in the mdx mouse restored by stem cell transplantation. Nature *401*, 390–394.

[6] Qu-Petersen, Z., Deasy, B., Jankowski, R., Ikezawa, M., Cummins, J., Pruchnic, R., Mytinger, J., Cao, B., Gates, C., Wernig, A., et al. (2002). Identification of a novel population of muscle stem cells in mice: potential for muscle regeneration. J. Cell Biol. *157*, 851–864.

[7] Corbel, S. Y., Lee, A., Yi, L., Duenas, J., Brazelton, T. R., Blau, H. M., and Rossi, F. M. (2003). Contribution of hematopoietic stem cells to skeletal muscle. Nat. Med. *9*, 1528–1532.

[8] Dezawa, M., Ishikawa, H., Itokazu, Y., Yoshihara, T., Hoshino, M., Takeda, S., Ide, C., and Nabeshima, Y. (2005). Bone marrow stromal cells generate muscle cells and repair muscle degeneration. Science *309*, 314–317.

[9] Sampaolesi, M., Blot, S., D'Antona, G., Granger, N., Tonlorenzi, R., Innocenzi, A., Mognol, P., Thibaud, J. L., Galvez, B. G., Barthelemy, I., et al. (2006). Mesoangioblast stem cells ameliorate muscle function in dystrophic dogs. Nature *444,* 574–579.

[10] Zhang, Y., Zhu, Y., Li, Y., Cao, J., Zhang, H., Chen, M., Wang, L., and Zhang, C. (2015). Long-term engraftment of myogenic progenitors from adipose-derived stem cells and muscle regeneration in dystrophic mice. Hum. Mol. Genet. *24*, 6029–6040.

[11] Fujita, R., Tamai, K., Aikawa, E., Nimura, K., Ishino, S., Kikuchi, Y., and Kaneda, Y. (2015). Endogenous mesenchymal stromal cells in bone marrow are required to preserve muscle function in mdx mice. Stem Cells *33*, 962–975.

[12] Hoffman, E. P., Brown, R. H., and Kunkel, L. M. (1987). Dystrophin: the protein product of the Duchenne Muscular Dystrophy locus. Cell *51*, 919–928.

[13] Briggs, D., and Morgan, J. E. (2013). Recent progress in satellite cell/myoblast engraftment: relevance for therapy. FEBS J. *280*, 4281–4293.

[14] Negroni, E., Gidaro, T., Bigot, A., Butler-Browne, G. S., Mouly, V., and Trollet, C. (2015). Invited review: Stem cells and muscle diseases: advances in cell therapy strategies. Neuropathol. Appl. Neurobiol. *41*, 270–287.

[15] Lapidos, K. A., Chen, Y. E., Earley, J. U., Heydemann, A., Huber, J. M., Chien, M., Ma, A., and McNally, E. M. (2004). Transplanted hematopoietic stem cells demonstrate impaired sarcoglycan expression after engraftment into cardiac and skeletal muscle. J. Clin. Invest. *114*, 1577–1585.

[16] Montarras, D., Morgan, J., Collins, C., Relaix, F., Zaffran, S., Cumano, A., Partridge, T., and Buckingham, M. (2005). Direct isolation of satellite cells for skeletal muscle regeneration. Science *309*, 2064–2067.

[17] Cerletti, M., Jurga, S., Witczak, C. A., Hirshman, M. F., Shadrach, J. L., Goodyear, L. J., and Wagers, A. J. (2008). Highly efficient, functional engraftment of skeletal muscle stem cells in dystrophic muscles. Cell *134*, 37–47.

[18] Tanaka, K. K., Hall, J. K., Troy, A. A., Cornelison, D. D., Majka, S. M., and Olwin, B. B. (2009). Syndecan-4-expressing muscle progenitor cells in the SP engraft as satellite cells during muscle regeneration. Cell Stem Cell *4*, 217–225.

[19] Gang, E. J., Darabi, R., Bosnakovski, D., Xu, Z., Kamm, K. E., Kyba, M., and Perlingeiro, R. C. (2009). Engraftment of mesenchymal stem cells into dystrophin-deficient mice is not accompanied by functional recovery. Exp. Cell Res. *315*, 2624–2636.

[20] Darabi, R., Gehlbach, K., Bachoo, R. M., Kamath, S., Osawa, M., Kamm, K. E., Kyba, M., and Perlingeiro, R. C. (2008). Functional skeletal muscle regeneration from differentiating embryonic stem cells. Nat. Med. *14*, 134–143.

[21] Davies, K. E., and Grounds, M. D. (2006). Treating muscular dystrophy with stem cells? Cell *127*, 1304–1306.

[22] Partridge, T. (2008) Denominator problems in a muscle stem cell study? Cell *135*, 997–998.

[23] Weiss, S. W., and Goldblum, J. R. (2001). Enzinger and Weiss's soft tissue tumors. (Mosby, London).

[24] Hendrix, M. J., Seftor, E. A., Seftor, R. E., Kasemeier-Kulesa, J., Kulesa, P. M., and Postovit, L. M. (2007). Reprogramming metastatic tumour cells with embryonic microenvironments. Nat. Rev. Cancer *7*, 246–255.

[25] Richler, C., and Yaffe, D. (1970). The in vitro cultivation and differentiation capacities of myogenic cell lines. Dev. Biol. *23*, 1–22.

[26] Rando, T. A., and Blau, H. M. (1994). Primary mouse myoblast purification, characterization, and transplantation for cell-mediated gene therapy. J. Cell Biol. *125*, 1275–1287.

[27] Delaporte, C., Dautreaux, B., and Fardeau, M. (1986). Human myotube differentiation in vitro in different culture conditions. Biol. Cell *57*, 17–22.

[28] Lendahl, U., Zimmerman, L. B., and McKay, R. D. (1990). CNS stem cells express a new class of intermediate filament protein. Cell *60*, 585–595.

[29] Goulding, M., Lumsden, A., and Paquette, A. J. (1994). Regulation of Pax-3 expression in the dermomyotome and its role in muscle development. Development *120*, 957–971.

[30] Murphy, M., and Kardon, G. (2011). Origin of vertebrate limb muscle: the role of progenitor and myoblast populations. Curr. Top Dev. Biol. *96*, 1–32.

[31] Buckingham, M., and Relaix, F. (2015). PAX3 and PAX7 as upstream regulators of myogenesis. *44*, 115–125.

[32] Plaks, V., Kong, N., and Werb, Z. (2015). The cancer stem cell niche: how essential is the niche in regulating stemness of tumor cells? Cell Stem Cell *16*, 225–238.

[33] Bonner, P. H., and Hauschka, S. D. (1974). Clonal analysis of vertebrate myogenesis: I. Early developmental events in the chick limb. Dev. Biol. *37*, 317–328.

[34] Stockdale, F. E. (1992). Myogenic cell lineages. Del. Biol. *154*, 284–298.

[35] Cho, M., Webster, S. G., and Blau, H. M. (1993). Evidence for myoblast-extrinsic regulation of slow myosin heavy chain expression during muscle fiber formation in embryonic development. J. Cell Biol. *121*, 795–810.

[36] Maximow, A. A., and Bloom, W. (1948). A text book of histology. (W.B. Saunders Company, Philadelphia), pp.167–171.

[37] Schmalbruch, H. (1976). The morphology of regeneration of skeletal muscles in the rat. Tissue Cell *8*, 673–692.

[38] Morgan, J. E., Pagel, C. N., Sherratt, T., and Partridge, T. A. (1993). Long-term persistence and migration of myogenic cells injected into pre-irradiated muscles of mdx mice. J. Neurol. Sci. *115*, 191–200.

[39] Pin, C. L., and Merrifield, P. A. (1997). Developmental potential of rat L6 myoblasts in vivo following injection into regenerating muscles. Dev. Biol. *188*, 147–166.

[40] Cornelison, D. D., and Wold, B. J. (1997). Single-cell analysis of regulatory gene expression in quiescent and activated mouse skeletal muscle satellite cells. Dev. Boil. *191*, 270–283.

[41] Zhao, P., and Hoffman, E. P. (2004). Embryonic myogenesis pathways in muscle regerenation. Dev. Dyn. *229*, 380–392.

[42] Coulton, G. R., Morgan, J. E., Partridge, T. A., and Sloper, J. C. (1988). The mdx mouse skeletal muscle myopathy: I. A histological, morphometric and biochemical investigation. Neuropathol. Appl. Neurobiol. *14*, 53–70.

[43] Xu, X., Wilschut, K. J., Kouklis, G., Tian, H., Hesse, R., Garland, C., Sbitany, H., Seth, R., Knott, P. D., Hoffman, W. Y., et al. (2015). Human satellite cell transplantation and regeneration from diverse skeletal muscles. Stem Cell Reports *5*, 419–434.

[44] Dellavalle, A., Sampaolesi, M., Tonlorenzi, R., Tagliafico, E., Sacchetti, B., Perani, L., Innocenzi, A., Galvez, B. G., Messina, G., Morosetti, R., et al. (2007). Pericytes of human skeletal muscle are myogenic precursors distinct from satellite cells. Nat. Cell Biol. *9*, 255–267.

[45] Mitchell, K. J., Pannerec, A., Cadot, B., Parlakian, A., Besson, V., Gomes, E. R., Marazzi, G., and Sassoon, D. A. (2010). Identification and characterization of a non-satellite cell muscle resident progenitor during postnatal development. Nat. Cell Biol. *12*, 257–266.

[46] Kostallari, E., Baba-Amer, Y., Alonso-Martin, S., Ngoh, P., Relaix, F., Lafuste, P., and Gherardi, R. K. (2015). Pericytes in the myovascular niche promote post-natal myofiber growth and satellite cell quiescence. Development *124*, 1242–1253.

[47] Lepper, C., Conway, S. J., and Fan, C. M. (2009). Adult satellite cells and embryonic muscle progenitors have distinct genetic requirements. Nature *460*, 627–631.

[48] Neal, A., Boldrin, L., and Morgan, J. E. (2012). The satellite cell in male and female, developing and adult mouse muscle: distinct stem cells for growth and regeneration. PLoS One *7*, e37950.

[49] Seale, P., Sabourin, L. A., Girgis-Gabardo, A., Mansouri, A., Gruss, P., and Rudnicki, M. A. (2000). Pax7 is required for the specification of myogenic satellite cells. Cell *102*, 777–786.

[50] Romero-Ramos, M., Vourc'h, P., Young, H. E., Lucas, P. A., Wu, Y., Chivatakarn, O., Zaman, R., Dunkelman, N., el-Kalay, M. A., and Chesselet, M. F. (2002). Neuronal differentiation of stem cells isolated from adult muscle. J. Neurosci. Res. *69*, 894–907.

[51] Arsic, N., Mamaeva, D., Lamb, N. J., and Fernandez, A. (2008). Muscle-derived stem cells isolated as non-adherent population give rise to cardiac, skeletal muscle and neural lineages. Exp. Cell Res. *314*, 1266–1280.

[52] Chanas-Sacre, G., Rogister, B., Moonen, G., and Leprince, P. (2000). Radial glia phenotype: origin, regulation, and transdifferentiation. J. Neurosci. Res. *61*, 357–363.

[53] Boldrin, L., Zammit, P. S., and Morgan, J. E. (2014). Satellite cells from dystrophic muscle retain regenerative capacity. Stem Cell Res. *14*, 20–29.

[54] Dubowitz, V. (1985). Muscle biopsy: A practical approach. (Bailliere Tindall, London), pp. 294.

[55] Karpati, G., Carpenter, S., and Prescott, S. (1988). Small-caliber skeletal muscle fibers do not suffer necrosis in mdx mouse dystrophy. Muscle Nerve *11*, 795–803.

[56] Blau, H. M., Webster, C., and Pavlath, G. K. (1983). Defective myoblasts identified in Duchenne muscular dystrophy. Proc. Natl. Acad. Sci. USA *80*, 4856–4860.

[57] Delaporte, C., Dehaupas, M., Fardeau, M. (1984). Comparison between the growth pattern of cell cultures from normal and Duchenne dystrophy muscle. J. Neurol. Sci. *64*, 149–160.

[58] Maier, F., and Bornemann, A. (1999). Comparison of the muscle fiber diameter and satellite cell frequency in human muscle biopsies. Muscle Nerve *22*, 578–583.

[59] Yokota, T., Lu, Q. L., Morgan, J. E., Davies, K. E., Fisher, R., Takeda, S., and Partridge, T. A. (2006). Expansion of revertant fibers in dystrophic mdx muscles reflects activity of muscle precursor cells and serves as an index of muscle regeneration. J. Cell Sci. *119,* 2679–2687.

[60] Schiaffino, S., Gorza, L., Pitton, G., Saggin, L., Ausoni, S., Sartore, S., and Lømo, T. (1988). Embryonic and neonatal myosin heavy chain in denervated and paralyzed rat skeletal muscle. Dev. Biol. *127*, 1–11.